ROTOR RESPONSE FOR TRANSIENT UNBALANCE CHANGES IN A NONLINEAR SIMULATION

M. J. Hine, C. E. Landis,
and R. F. Beatty

Abstract

Synchronous rotor response varies significantly with transient unbalance distribution and speed simultaneously. In addition to this response variation, the complexity of a nonlinear rotor system can alter the response and produce nonsynchronous motion. A transient unbalance phenomena created a concern about a perturbation source for unstable operation. As an outgrowth of the Dynamic Balance Improvement Study Phase II contract with NASA/MSFC, transient unbalance shifts have been determined not to excite a rotor instability in the high pressure turbomachinery of the Space Shuttle Main Engine using the current rotordynamic models. Sudden unbalance changes of relatively small magnitudes during fast-speed ramps have shown stable nonsynchronous motion depending on the resultant unbalance distribution at subsequent high speed dwells. Transient moment unbalance may initiate a limit cycle subsynchronous response that shortly decays, but a persistent subsynchronous with large amplitudes was never achieved. These limit cycle subsynchronous amplitudes appear to be minimized with lower unbalance magnitudes, which indicates improved rotor balancing would sustain synchronous motion only. The transient unbalance phenomenon was determined to be an explanation for synchronous response shifts often observed during engine tests.

Introduction

Throttleable pump-fed liquid rocket engines require variable speed turbopumps capable of fast-speed ramp rates. A high rate of change in the applied torque may cause rotor components to reposition and alter the rotor mass unbalance. This concern, along with other possible unbalance changing mechanisms,

was expressed as a self-enhanced unbalance concern by NASA. It was suggested that transient unbalance changes could initiate an asynchronous rotor instability close to the spin frequency. The focus of concern was with the high performance turbopumps of the Space Shuttle Main Engine (SSME). The SSME powerhead with the main combustion elements and attached turbopumps is shown in Fig. 1. The throttleable SSME has high

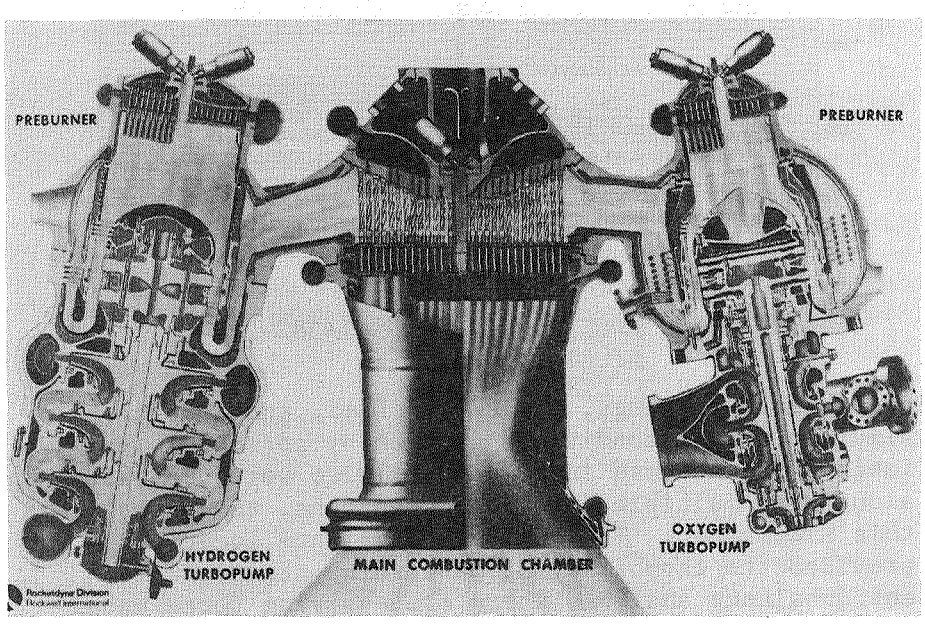

Fig. 1. SSME Powerhead Component Arrangement

pressure liquid oxygen and liquid hydrogen turbopumps, which have had stability problems in the past, and this transient unbalance mechanism was investigated as a technology item. The primary concern for this phenomenon was an initiation mechanism for a roughly 90 percent of speed subsynchronous whirl on the high pressure oxygen turbopump. Test data would normally indicate this subsynchronous response at the maximum shaft speed, or directly after a speed ramp, as shown in the example frequency versus time data plot of Fig. 2.

To perform this complex transient analysis, nonlinear models were required and included such effects

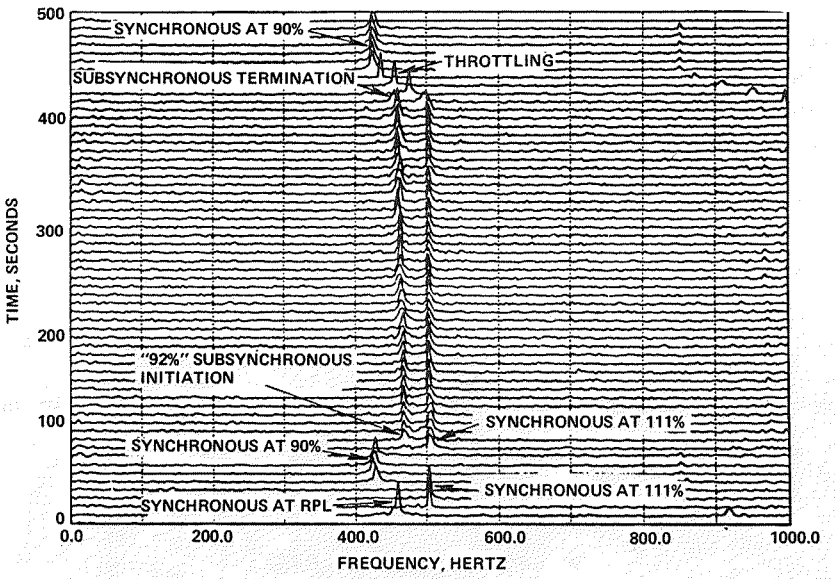

Fig. 2. HPOTP 2212 Test 901-382-2214 Accelerometer Data

as deadband bearings, fixed sideload, and rubbing to simulate actual conditions as much as possible. Variable unbalance and speed capabilities were necessary, along with multiple unbalance locations, to accomplish this simulation. The multiple unbalance locations provided the capability of performing transient moment unbalance analyses where time-varying force unbalance magnitudes on adjacent turbine disks form a variable couple. These conditions require unique simulation programming and would generally create a large computer cost. However, hybrid computer usage made it possible to perform the analysis for a minimal cost and significant time savings.

Survey Turbopumps

The existing nonlinear simulation models of the high pressure oxygen turbopump (HPOTP) and high pressure fuel (liquid hydrogen) turbopump (HPFTP) were used to perform the analysis. The following is a brief description of these turbopumps.

The high pressure oxidizer turbopump is shown in Fig. 3 and a summary of its performance characteristics are provided in Table 1. Basically, the high pressure

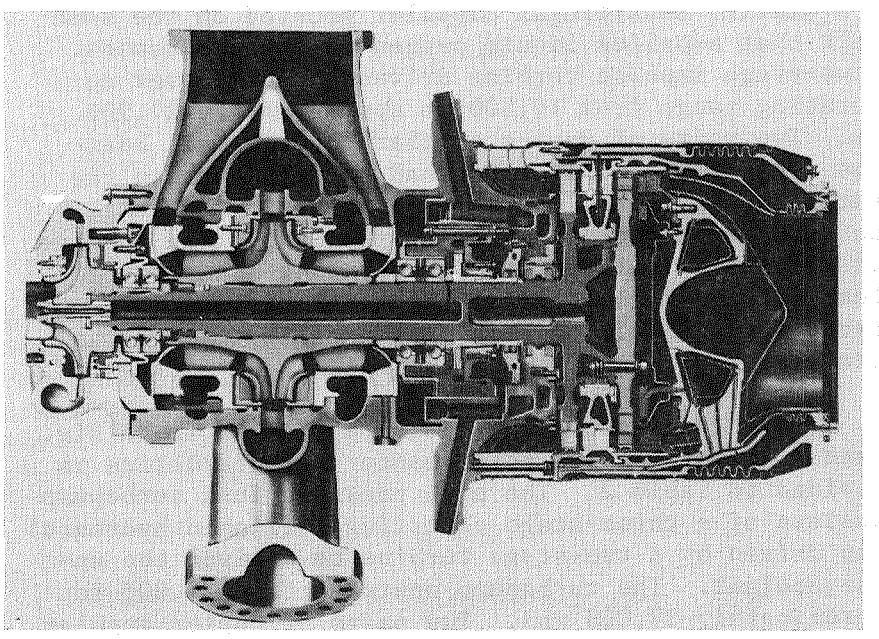

Fig. 3. SSME High Pressure Oxidizer Turbopump

Table 1. SSME HPOTP Performance Data

KEY PERFORMANCE PARAMETERS BASELINE DATA JAN. 1984				
	RPL		FPL	
	MAIN	BOOST	MAIN	BOOST
PUMP INLET FLOWRATE, LB/SEC	1070.6	111.6	1157.8	129.4
PUMP INLET PRESS, PSIA	379.3	3985.9	392.4	4403.6
PUMP DISCHARGE PRESSURE, PSIA	4108.7	7106.7	4556.0	7861.2
PUMP EFFICIENCY	0.684	0.809	0.650	0.800
TURBINE FLOWRATE, LB/SEC	61.8		69.0	
TURBINE INLET PRESSURE, PSIA	5015.3		5660.8	
TURBINE INLET TEMP, R	1407.2		1596.3	
TURBINE PRESS RATIO	1.506		1.550	
TURBINE EFFICIENCY	0.749		0.755	
TURBINE SPEED, RPM	27102		29675	
TURBINE HORSEPOWER	22902		29174	

oxidizer turbopump consists of a double-entry centrifugal impeller supplying liquid oxygen to the main chamber. A portion of this discharge flow is diverted to a smaller centrifugal impeller mounted on the same shaft that supplies liquid oxygen to the preburners. A two-stage impulse turbine drives the pump over an operating range from 19,500 to approximately 27,900 rpm. Two pairs of duplex angular contact ball bearings support the rotor. Preload springs between the bearing outer races in each pair maintain the axial load independent of rotor axial position. The turbine hot gases are isolated from the pump by a series of floating ring seals. Axial thrust on the rotor is reacted by a double balance piston built into the main impeller.

The high pressure fuel turbopump is shown in Fig. 4 and a summary of its performance characteristics is provided in Table 2. The high pressure fuel turbopump consists of a three-stage centrifugal (liquid hydrogen) pump driven by a two-stage turbine to deliver the engine coolant. The turbopump operates from 27,000 to approximately 37,000 rpm. Two pairs of duplex angular

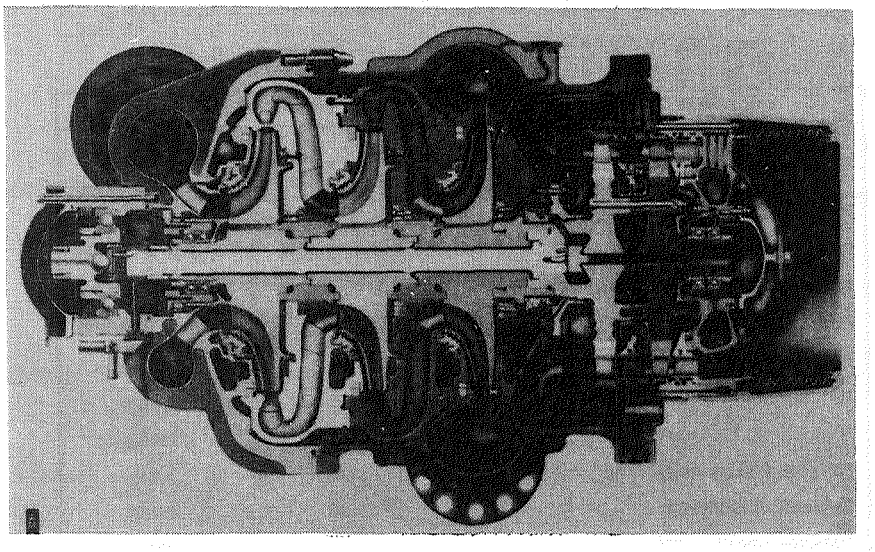

Fig. 4. SSME High Presure Fuel Turbopump

Table 2. SSME HPFTP Performance Data

KEY PERFORMANCE PARAMETERS	RPL	FPL
PUMP INLET FLOWRATE, LB/SEC	148.4	161.7
PUMP INLET PRESSURE, PSIA	204.1	214.0
PUMP DISCHARGE PRESSURE, PSIA	6254.8	7036.8
PUMP EFFICIENCY	0.758	0.757
TURBINE FLOWRATE, LB/SEC	147.5	164.0
TURBINE INLET TEMPERATURE, R	1898.4	1989.2
TURBINE PRESSURE RATIO	1.522	1.558
TURBINE EFFICIENCY	0.770	0.780
TURBINE SPEED, RPM	34,931	37,076
TURBINE HORSEPOWER	63,288	77,142

contact ball bearings support the rotor radially and a thrust bearing is provided for start and shutdown axial positioning. A balance piston built into the third-stage impeller reacts the axial thrust during steady-state operation. Straight smooth annular seals between the impeller stages ensure the rotor stability.

Mathematical Models Description

The finite element models of the rotors and housings for the high pressure oxidizer and fuel turbopumps have been verified by years of empirical correlation and are generally accepted as producing the correct trends. The rotors are constructed of beam finite elements and the load line diagrams are shown in Fig. 5 and 6 for the high pressure oxidizer and fuel turbopumps, respectively. The high pressure oxidizer turbopump housing model, shown in Fig. 7, is constructed of plate elements and equivalent support beams that tie the housing to the engine chamber ground. The high pressure fuel turbopump housing model, shown in Fig. 8, is of beam and empirically sized spring construction, which is also tied to the engine chamber ground. The coupled system was analyzed using modal synthesis techniques that combine substructures of the rotor and housing-to-engine

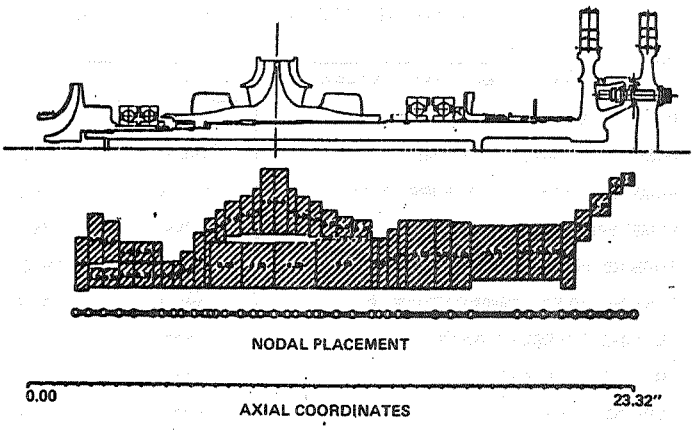

Fig. 5. SSME HPOTP Rotating Assembly Finite Element Model

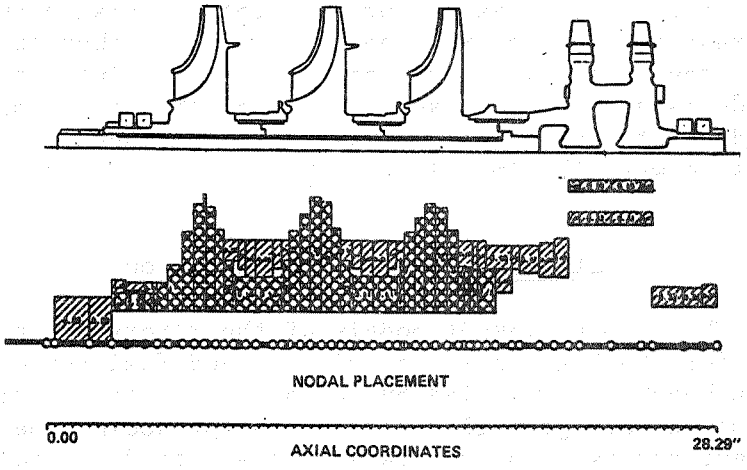

Fig. 6. SSME HPFTP Rotating Assembly Finite Element Model

support structure coupled through nonlinear bearings, hydrostatic seals, impeller-diffuser interaction, turbine aerodynamic cross-coupling, bearing damping, and fixed radial loads. Output capabilities include the ability to predict bearing loads, rotor displacements, and housing accelerations as a function of time and speed, and determine the response spectra.

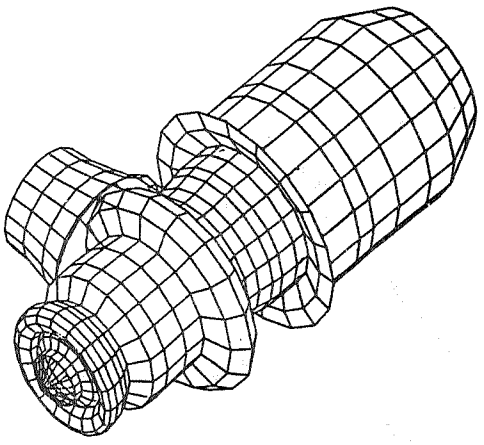

Fig. 7. SSME HPOTP Housing Finite Element Model

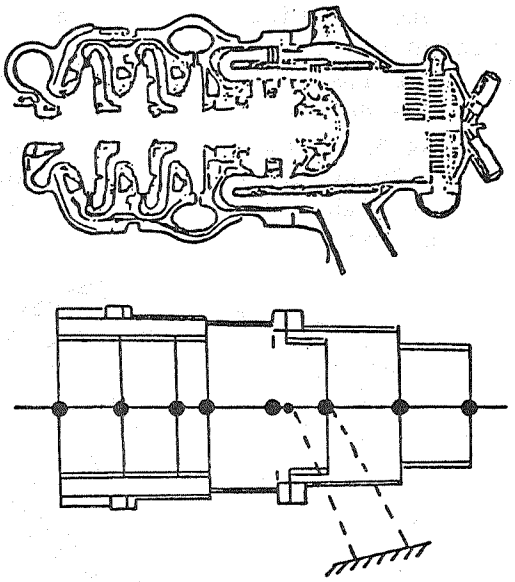

Fig. 8. SSME HPFTP Housing Model

The high pressure oxidizer turbopump operates between its first and second rotor critical speeds at approximately 12,000 and 32,500 rpm, respectively. The lowest rotor critical speed is the turbine overhang mode and is shown in Fig. 9. The higher rotor critical speed is the main impeller mode and is shown

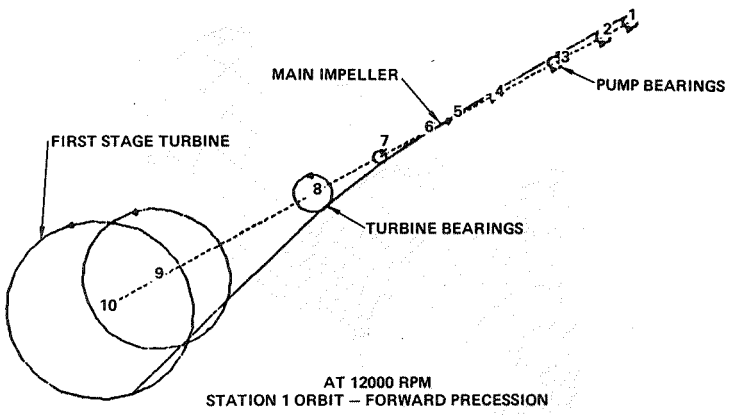

Fig. 9. SSME HPOTP Lowest Rotor Critical Turbine Overhang Mode

in Fig. 10. The high pressure fuel turbopump operates above its first rotor critical speed at about 17,000 rpm, but the second critical is in the speed range at approximately 32,000 rpm. The lower rotor mode has its maximum relative deflection approximately halfway between the bearing span and is shown in Fig. 11. The high pressure fuel turbopump 32,000 rpm rotor mode shown in Fig. 12 is highly damped by the straight smooth impeller interstage seals.

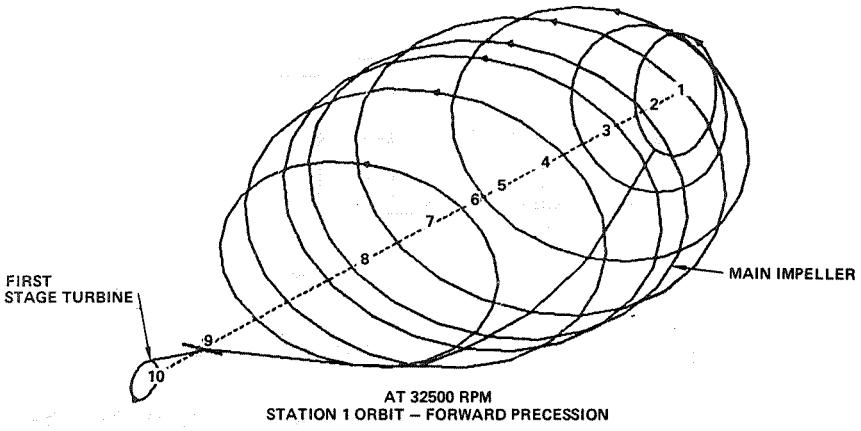

Fig. 10. SSME HPOTP Higher Rotor Critical Main Impeller Mode

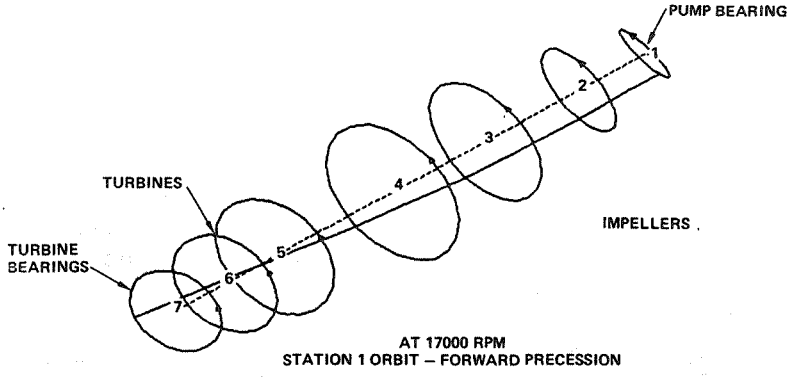

Fig. 11. SSME HPFTP Lowest Rotor Critical Skip Rope Mode

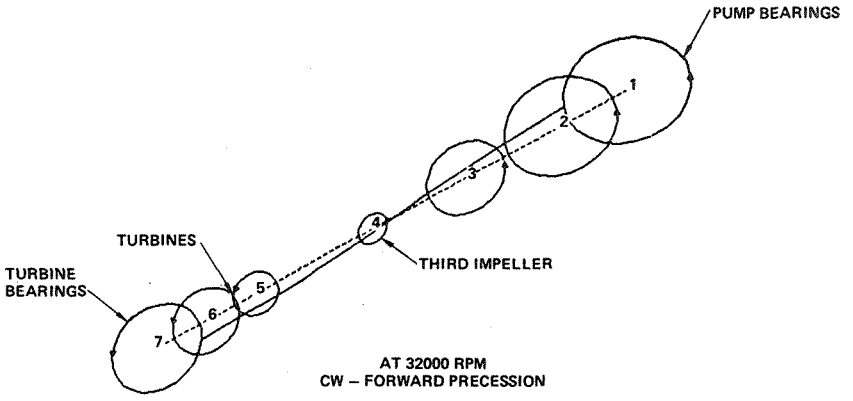

Fig. 12. SSME HPFTP Higher Rotor Mode Node at Third Impeller

Hybrid Model

These nonlinear rotordynamics models mechanized on an AD10 hybrid computer were used to study the transient unbalance changes. The hybrid computer allows the complete interactive operation of the model during these parametric studies.

Location, magnitude, and rate of change of the unbalances can be changed on-line and the resulting bearing loads and housing acceleration can be monitored on time-history brush charts. If, for example,

an undesirable unbalance was used, the analysis could be terminated immediately and new unbalance values entered for a repeat case. The time-history data from the hybrid model is digitally stored for post-processing to obtain spectral information.

A slight model modification had to be made to model time and speed varying unbalances since these variables were not normal parametric options of the model. To the best of our knowledge, Rocketdyne has the only time and speed variable unbalance analysis capability anywhere. To acquire this capability, an existing program option to simulate step unbalances at a discrete time was modified. This is mechanized as:

$$U = U_I \text{ if time} < t_u$$

$$U = U_I + U_s \text{ if time} \geq t_u$$

where

U = effective unbalance

U_I = constant unbalance

U_s = increase in unbalance at time t_u

t_u = time the step unbalance occurs

Graphically, this would look like Fig. 13.

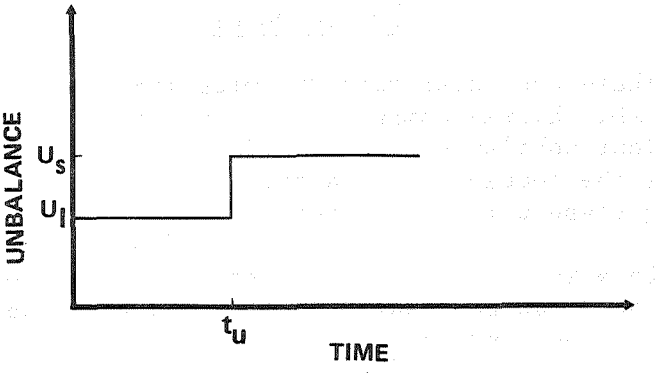

Fig. 13. Step Unbalance With Time

To simulate time and speed varying mechanisms, this was modified to:

$$U = U_I \text{ if time} < t_u$$
$$U = U_I + \dot{U}_s \text{ (time} - t_u) \text{ if } t_u \leq \text{time} \leq t_s$$
$$U = U_I + \dot{U}_s \ (t_s - t_u) \text{ if time} > t_s$$

where

$\dot{U}_s$ = rate of unbalance change, gm-in./sec

t_s = time the unbalance stops changing

Graphically, this appears as Fig. 14.

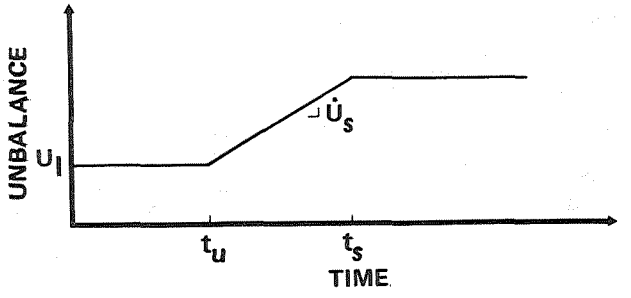

Fig. 14. Ramp Unbalance With Time

This mechanization permits complete flexibility in specifying the transient unbalance and also maintains the capability for simulating step unbalances.

Response Results

The initial state of balance in these simulations was established at all the major disks along both rotors based on build tolerances. Nominal state of balance conditions for the high pressure oxidizer and fuel turbopumps are shown in Fig. 15 and 16. It was determined for all self-enhanced unbalance mechanisms proposed that a significant unbalance change was not possible with the SSME turbopumps because splines, pilots, and normality tolerances were sufficient for maintaining rotor positioning. However, to study the

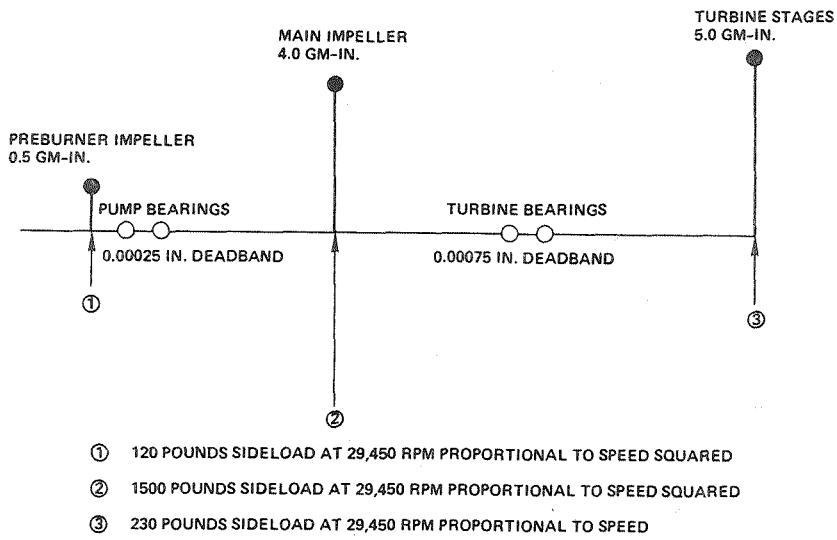

Fig. 15. HPOTP Model Initial Conditions

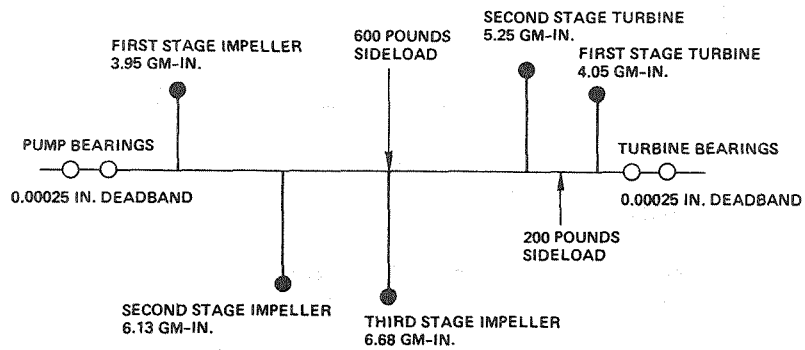

Fig. 16. HPFTP Model Initial Conditions

effect of changing unbalance for information only, it was arbitrarily decided to vary the unbalance magnitude by a factor of two over the speed ramp. Numerous simulations were performed with typically stable and well behaved synchronous only results. Some of the more interesting results will now be discussed.

HPFTP Time-Varying Unbalance

The unbalance at the first stage impeller was varied above and below the maximum anticipated

unbalance during an increasing speed ramp as in Fig. 17. The resultant acceleration response at the pump flange is shown in Fig. 18. All response parameters showed stable behavior following the ramp. Since the rotor unbalance distribution is altered, the rotor displacement constantly varies along the rotor length.

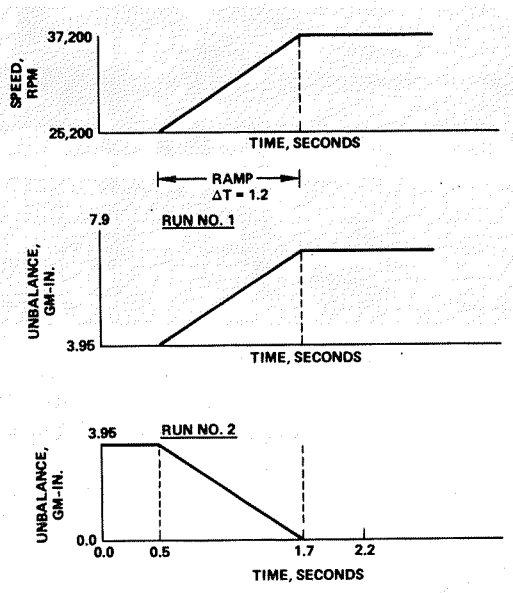

Fig. 17. HPFTP Computer (AD-10) Model Input for Time-Dependent Unbalance Increase and Decrease Applied at the First Impeller

HPFTP Time-Varying Moment

A transient moment was simulated by varying opposing unbalances at the first- and second-stage turbine disks above and below the maximum anticipated values during a speed ramp as in Fig. 19 and 20. The resultant acceleration response of the pump flange is shown in Fig. 21.

The pump appears to be basically unaffected by the moment changes themselves after the speed ramp. Following the speed ramp, for both increasing and decreasing turbine moment unbalance cases, a limit cycle subsynchronous response is present as shown in examples (Fig. 22 and 23) for a turbine bearing load and

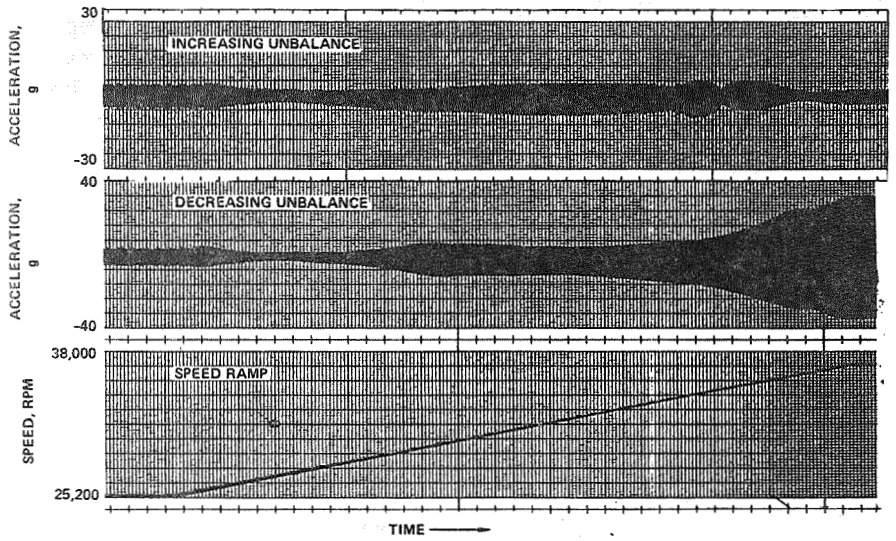

Fig. 18. HPFTP Housing Acceleration Response to Unbalance Changes at First Impeller

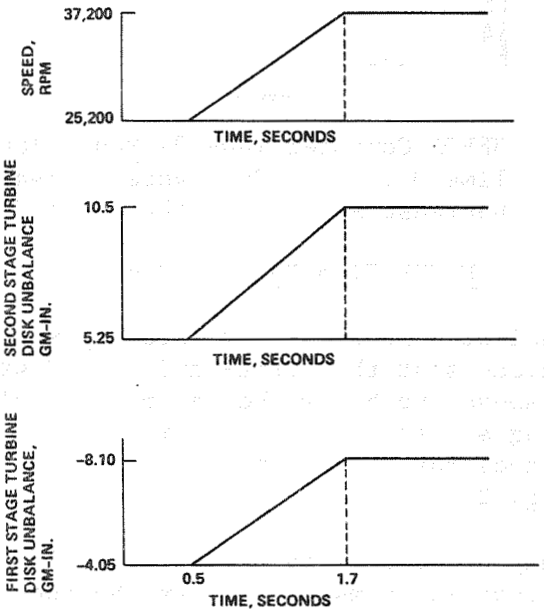

Fig. 19. HPFTP Computer (AD-10) Model Input for Time-Dependent Moment Unbalance Increase

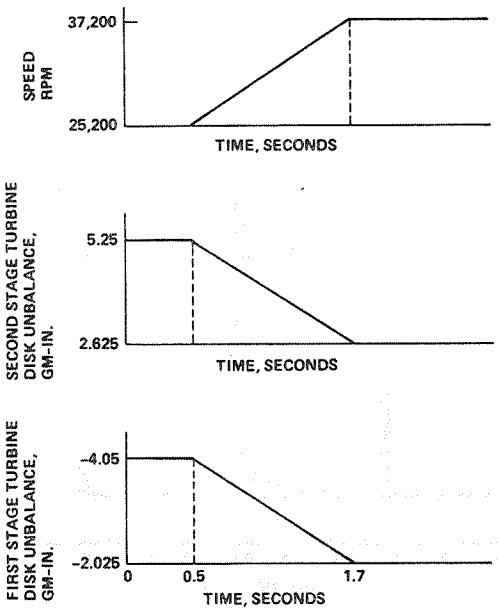

Fig. 20. HPFTP Computer (AD-10) Model Input for Time-Dependent Moment Unbalance Decrease

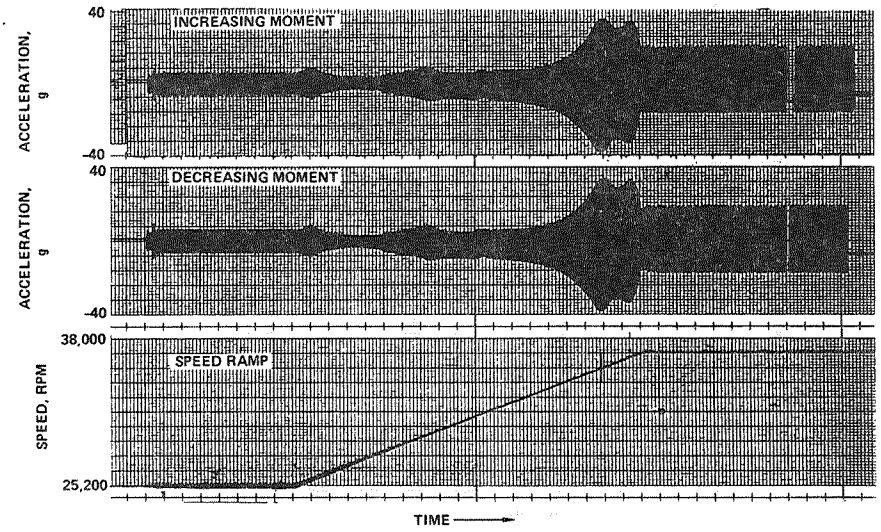

Fig. 21. HPFTP Housing Acceleration Response to Varying Moment Unbalance at Turbine

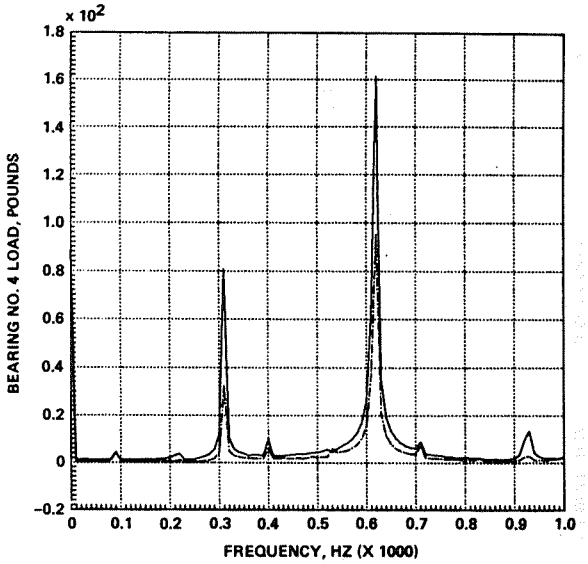

Fig. 22. HPFTP Spectra at 37,200 rpm with Increasing Moment Unbalance

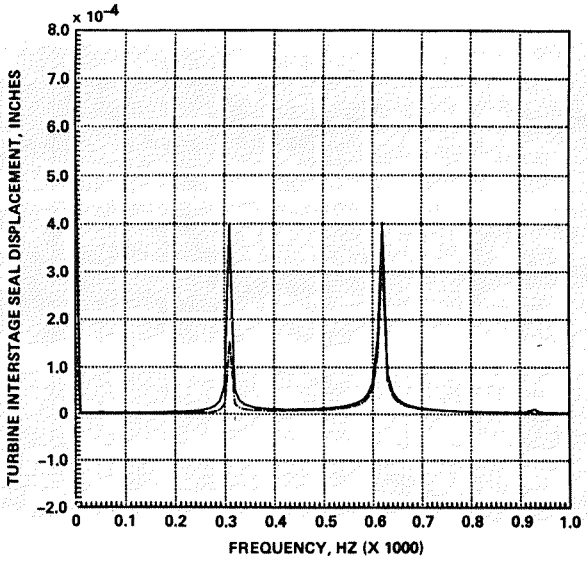

Fig. 23. HPFTP Spectra at 37,200 rpm with Increasing Moment Unbalance

turbine interstage seal displacement with an increasing moment unbalance. This lowest rotor mode subsynchronous response is attributed to the changes during the ramp since during normal operation at high speeds, the subsynchronous response is not present in the simulations. This level of subsynchronous response in the 300 Hz range is typically not experienced with a straight smooth impeller interstage seal configuration high pressure fuel turbopump during engine hot-fire testing. For normal steady-state unbalance distributions and high-speed dwell conditions, the typical response spectra is shown in Fig. 24, which the data represented in Fig. 22 and 23 eventually decays to reflect. Sensitivity to the initial conditions is typical in nonlinear simulation work.

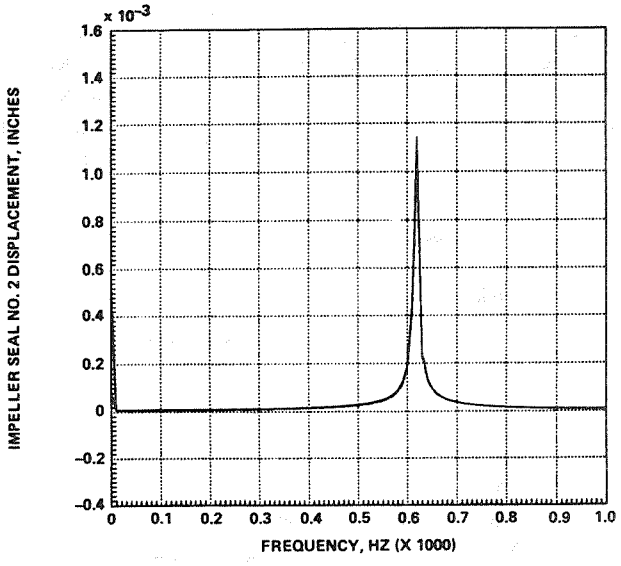

Fig. 24. Typical HPFTP Response Spectra at 37,200 rpm

HPOTP Time-Varying Unbalance

The effect on the rotor response of a time-varying unbalance during a speed ramp was studied with the unbalance occurring separately on the turbine and main impeller. Both increasing and decreasing unbalances were studied during a speed increasing ramp as

shown in Fig. 25 and 26. The acceleration of the housing flange is shown in Fig. 27 for the unbalance changes occurring at the main impeller. As expected, the increasing unbalance case produced larger residual response magnitudes than the decreasing case. The pump housing acceleration response to unbalance changes at the turbine is shown in Fig. 28.

The steady-state pump response was determined by the final unbalance magnitude and speed for the main impeller unbalance case. Variations in the response were observed during the speed ramp for the two analysis conditions where resonant activity was observed near the rotor critical speed and housing resonances.

The pump was dwelled at high speed for both unbalance conditions with subsynchronous activity at one-half synchronous speed, or the lowest rotor mode in the spectral displacement data at the turbine stages which was not present in the bearing loads or housing accelerations.

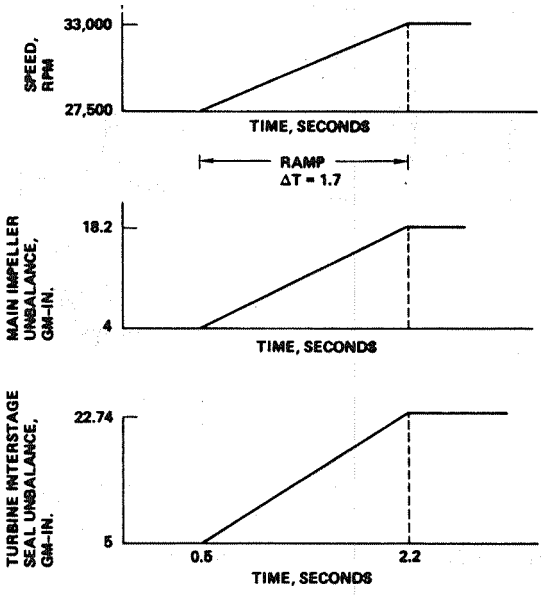

Fig. 25. HPOTP Computer (AD-10) Model Input for Time-Dependent Unbalance Increase

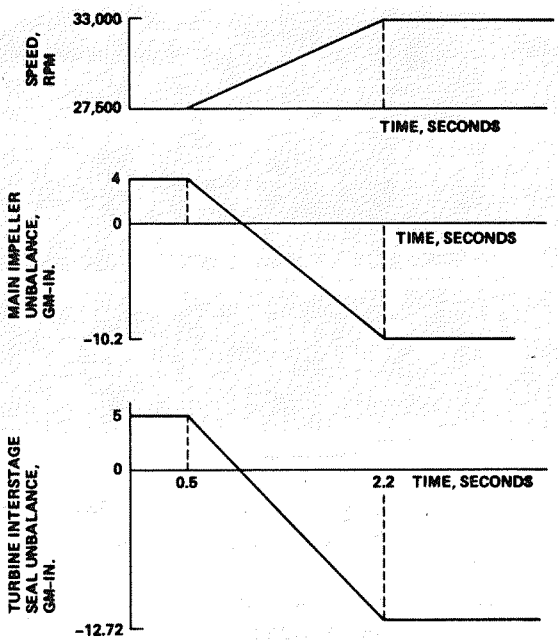

Fig. 26. HPOTP Computer (AD-10) Model Output for Time-Dependent Unbalance Decrease

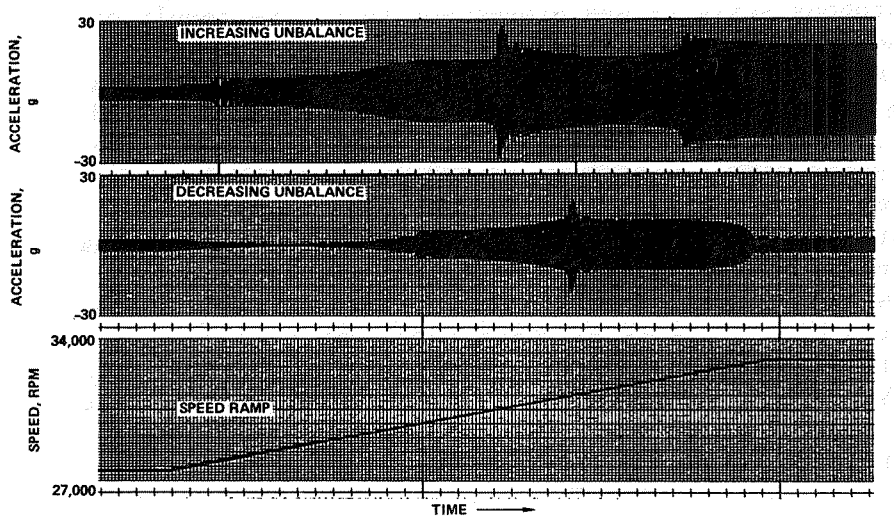

Fig. 27. HPOTP Housing Acceleration Response to Varying Unbalance at Main Impeller

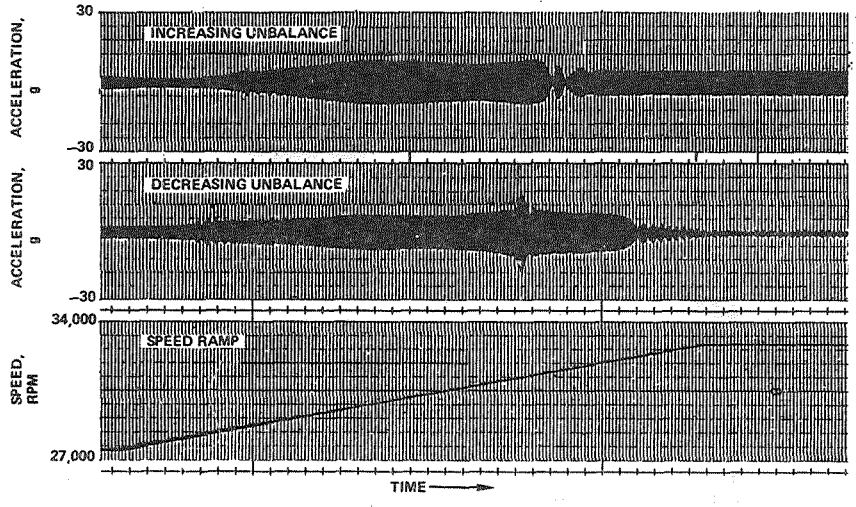

Fig. 28. HPOTP Housing Acceleration Response to Varying Unbalance at Turbine

Turbine response is shown in Fig. 29 and 30 for the increased and decreased main impeller unbalances, respectively. Of note here is that the subsynchronous amplitudes after an unbalance increase were higher than those after an unbalance decrease. This subsynchronous activity was proven not to be the result of the unbalance changes and speed ramp by operating at a constant speed of 33,000 rpm with the unbalance existing at the end of the speed ramp. Figures 31 and 32, respectively, show similar subsynchronous activity for high constant speed and similar unbalance conditions at the end of the ramps. It should be noted that 33,000 rpm is far in excess of the maximum running speed of 28,200 rpm at 104 percent of rated power. A modified turbine interstage seal for the uprated high pressure oxidizer turbopump (109 percent thrust) has been shown to eliminate the turbine disks subsynchronous response, even at this excessive speed as shown in Fig. 33. As previously mentioned, the subsynchronous response was never observed in the housing acceleration data, which is monitored on every engine hot-fire test and is a reflection of the bearing loads.

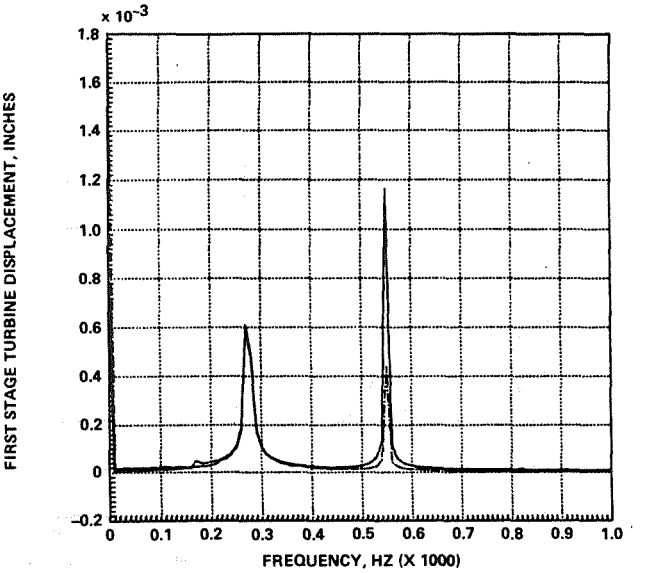

Fig. 29. HPOTP Increased Impeller Unbalance Response After Speed Ramp

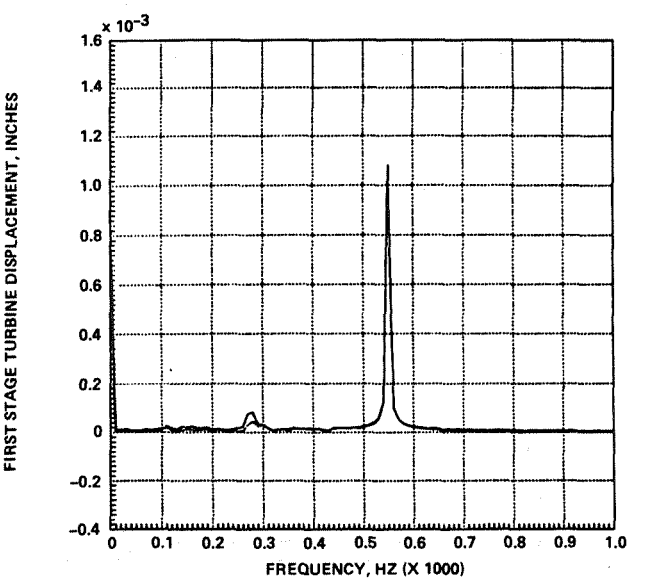

Fig. 30. HPOTP Decreased Impeller Unbalance Response After Speed Ramp

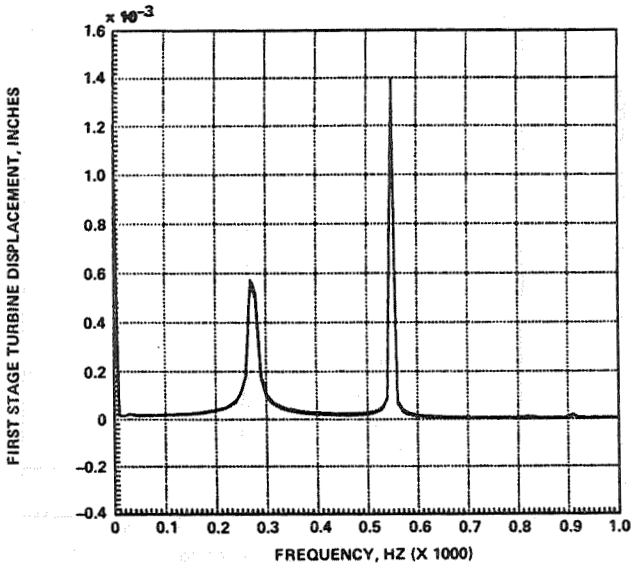

Fig. 31. HPOTP Response Spectra at 33,000 rpm Turbine Unbalance Increase

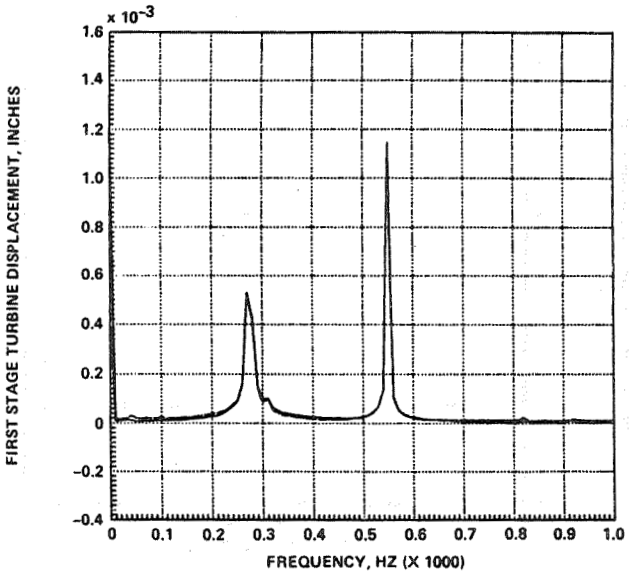

Fig. 32. HPOTP Response Spectra at 33,000 rpm Turbine Unbalance Decrease

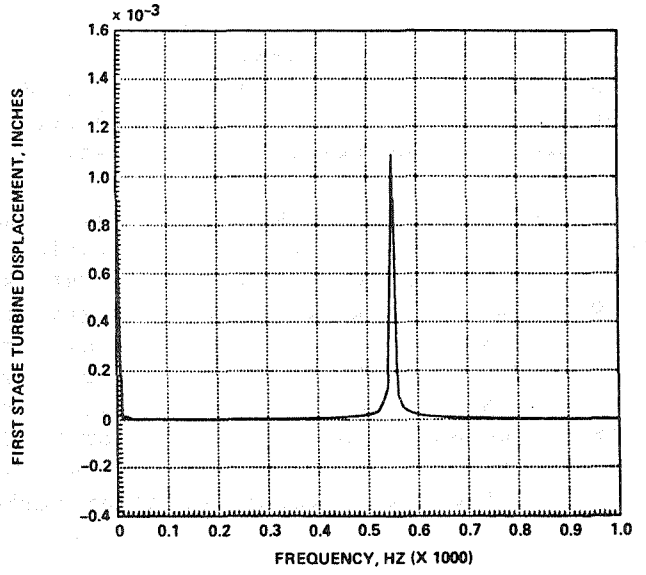

Fig. 33. Typical HPOTP Response Spectra at 33,000 rpm With Modified Turbine Interstage Seal

Conclusions

Numerous transient unbalance cases were performed on speed ramps and a divergent rotor instability, or nonsynchronous motion close to the operating speed, was never achieved. Unbalance changes in excess of reasonable analytically predicted magnitudes caused significant synchronous response variation due to the resulting unbalance distribution exciting different system modes. The limit cycle subsynchronous rotor motion detected for both turbopumps was always at the lowest rotor mode frequency, never at a higher rotor mode frequency. The lower rotor mode stability for either turbopump has not been a problem since well before the first Shuttle launch. The high pressure fuel turbopump subsynchronous rotor mode response was shown at a speed slightly above the maximum operating speed and has not been experienced during hot-fire testing since the conversion to straight smooth impeller interstage seals. The high pressure oxidizer

turbopump lowest rotor mode subsynchronous response is not present at speeds up to a maximum operating speed of 30,000 rpm and the low levels shown at 33,000 rpm can be suppressed with a turbine interstage seal modification currently in the development stages.

Lower transient unbalance magnitude shifts may explain some of the synchronous response variation occasionally seen during engine test or the "haystack" phenomenon observed in flight, which was a gradual increase in high pressure oxidizer turbopump synchronous response followed by a short decrease to the original levels. However, as a result of this study, a transient unbalance mechanism cannot explain, or be described as, the trigger for 90 percent of speed subsynchronous whirl on the high pressure oxidizer turbopump.